

Final Technical Report: Full-scale Experimental Validation of Dynamic, Centrifugally Powered, Pneumatic Actuators for Active Rotor Blade Surfaces

NASA Award Number: NNX13AB81A

Investigator(s): Dr. Joseph Szefti - Invercon LLC, Brian Cormier and Luke Ionno- Kaman Aerospace Corporation

Introduction

For several decades, the rotorcraft community has recognized the potential performance benefits that could be gained by incorporating active surfaces on rotor blades, particularly trailing edge flaps¹. Over the years, several researchers have detailed the vibration control benefits provided by flaps, while several also have envisioned rotors that rely on trailing edge flaps to provide primary control, thus completely eliminating the need for a mechanical swashplate assembly. Analytical investigations in the literature suggest that flap displacements of $\pm 15^\circ$ to $\pm 20^\circ$ are required to achieve swashplateless forward flight²⁻⁶. It must be noted that Kaman’s K-MAX helicopter already achieves primary control through the motion of servoflaps, although a mechanical linkage from the servoflap to the hub is still required to achieve the required servoflap motion.

Moreover, several researchers have attempted to realize flap motion through the use of on-blade actuators, mostly in the form piezoelectric-based and electromechanical devices. Both of these solutions, however, introduce a number of new blade and aircraft design issues. In the case of piezoelectric devices, the active PZT material is lead-based and has a similar density to steel. In addition, piezoelectric devices require an ancillary motion amplification system which also adds unwanted blade weight. Because of this added weight, blades must be reinforced in the area of installation to accommodate the increased centrifugal forces (CF) introduced by the system. On top of weight concerns, high voltage must be routed to the device through advanced electrical slip rings, and electrical amplifiers must be onboard to generate the actuator signals, adding more weight. Thus far, piezoelectric devices have also exhibited limited stroke in the range of $\pm 3^\circ$. More traditional, and often very complex, electromechanical design solutions also have similar unwanted added weight and slip ring issues and usually suffer from mechanical wear issues introduced by increased internal mechanism friction caused by extreme CF loading.

In the current work, Invercon has proposed a radical departure from these design concepts, one in which the actuator output is powered using an on-blade, centrifugally developed pressure differential, introducing extremely little blade weight. In Figure 1, a schematic illustrates this concept. It would be advantageous to utilize the large centripetal acceleration created by the rotor to generate an on-blade air pressure differential for actuation, thus eliminating both the need to transmit high amounts of electrical power to the rotating frame and the need for heavy, traditional actuators that can negatively impact

overall rotor blade weight. A conceptual schematic of a centrifugally powered pneumatic actuator that powers a trailing edge flap is pictured in Figure 2. Invercon’s actuation concept is directly aligned with the objectives of NASA’s Subsonic Rotary Wing Project, having the potential to enable more efficient flight, enhance vehicle maneuverability, allow for multi-mission vehicle configurations, reduce exterior noise, and generally enhance the competitiveness of US rotary winged vehicles in the civil sector.

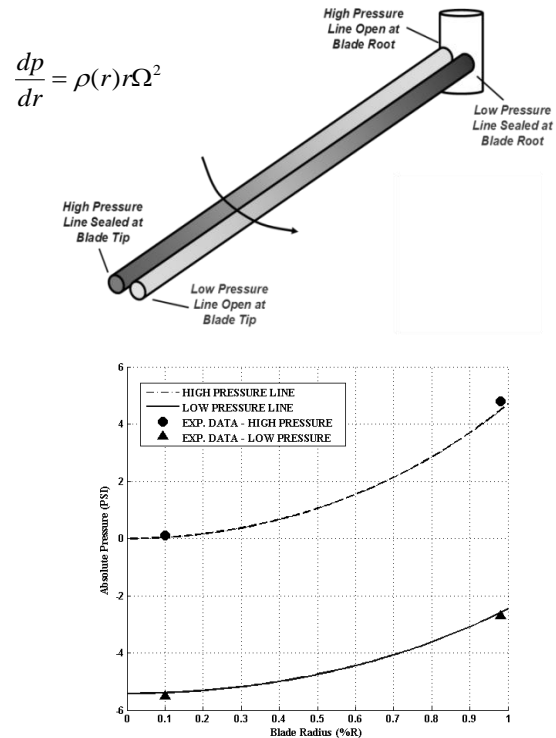


Figure 1. a) Schematic of Invercon’s centrifugally generated pressure differential concept for actuation, and b) predicted pressure and experimentally measured pressure values (280 RPM, 24 ft. radius rotor)

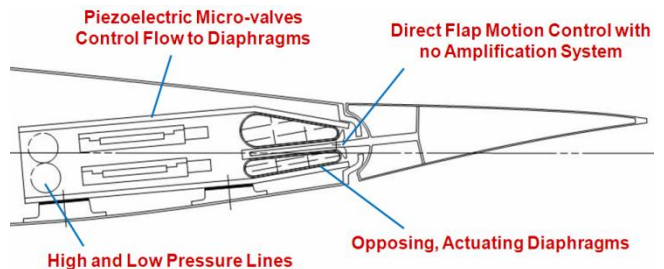


Figure 2. Conceptual centrifugally powered pneumatic actuator powering a trailing edge flap

Objectives

The objectives this Phase I program were 1) to experimentally demonstrate a revolutionary active rotor actuation concept on a full scale rotor: centrifugally powered, pneumatic actuation for rotor blade active surfaces 2) to compare experimental results to analytical performance predictions of pneumatic actuation, and 3) to determine the viability of pneumatic actuation of various active surface concepts, particularly trailing edge flaps, through full-scale demonstration of this new concept.

Approach

In order to achieve the project objectives, the following tasks were performed. First, Invercon and Kaman secured a set of retired K-MAX blades for modification to house the centrifugally generated pressure lines and the pneumatic actuator. Invercon then designed and fabricated a representative pneumatic actuator that could be installed in the K-MAX blade. Upon successful bench testing of the actuator, Invercon and Kaman then installed the actuator in the K-MAX blade. Subsequently, full-scale spin testing of the pneumatic actuator powered by centrifugally generated pressures was performed in Fall, 2013, at Kaman’s whirl rig facility, and the processed test results were then analyzed. An additional task was added to the spin test matrix, which was the experimental demonstration of power harvesting using the centrifugally generated pressure differential. It was shown that the amount of power that could be harvested using the pressure differential will provide sufficient power for not only pneumatic valve actuation, but also for blade sensing and wireless control data transmission in future rotorcraft without the need for an electromechanical slip ring. Finally, a state space model of the pneumatic actuation system was developed and analytical and experimental results were compared to validate the model. The validated model was then used to assess the actuator’s potential to power active trailing edge flaps.

Accomplishments

- Secured K911009 K-MAX blades for testing.
- Designed blade modifications to allow for actuator testing while maintaining blade structural integrity during spin testing.
- Designed and spin tested three-way piezoelectric valves suitable for actuator while under CF loading.
- Designed pneumatic actuator and actuator housing
- Modified blades to house pneumatic actuator
- Installed actuator in blade and successfully conducted actuator spin testing at Kaman’s whirl rig
- Performed pneumatic power harvesting spin testing
- Developed and validated state space model capturing pneumatic actuator/flap dynamics
- Analytically demonstrated pneumatic actuators capable of powering full-scale trailing edge flaps for vibration control and primary rotor control

K-MAX Test Blades

Early in the Phase I effort, Kaman secured a set of K911009 K-MAX blades to be modified for pneumatic actuator spin testing, pictured in Figure 3. CAD drawings of the blades were provided to Invercon for pneumatic actuator design integration.



Figure 3. K911009 Blades Secured for Spin Testing

Blade Modification Specifications

Subsequently, Invercon and Kaman collaborated to determine a suitable location to house the pneumatic actuator in the blade and also an appropriate method to modify the blades in order to span pneumatic lines from the blade root to the actuator housing, and from the actuator housing to the blade tip. Subsequently, a comprehensive actuator specification document was generated by Kaman to aid in the actuator’s design and integration. It was decided that Invercon’s pneumatic actuator assembly and structural support housing must be designed to fit entirely within the definition of the K911009 Control Box. A reference planform view of the generalized location of the K911009 Control Box and ISO view of the control box is shown in Figure 4. As a reference dimension, the area is approximately 12.06 inches in length and 4.40 inches in width, and its height follows the contour of the control box.

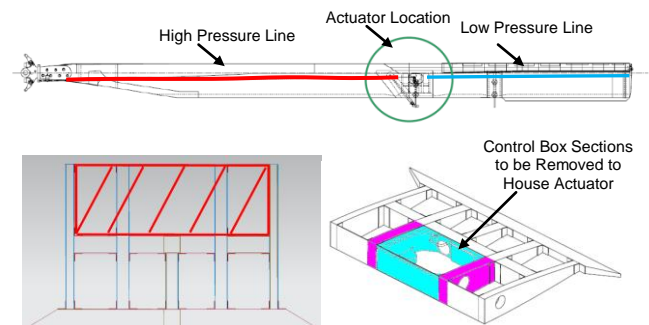


Figure 4. View of K911009 control box area modifications and location of pneumatic supply lines

Piezoelectric Valve Design and Testing

Invercon then designed, fabricated, and spin tested lightweight, three-way piezoelectric valves to be used in the actuator design. The valves were designed to operate with up to a 10 psi pressure differential. To ensure that the valves would be able to operate under 500 g’s of centrifugal loading (spin testing conditions), Invercon utilized a modified centrifuge test stand that is capable of pressure testing under varying rotating speeds. The valve schematic and centrifuge test stand are pictured in Figure 5.

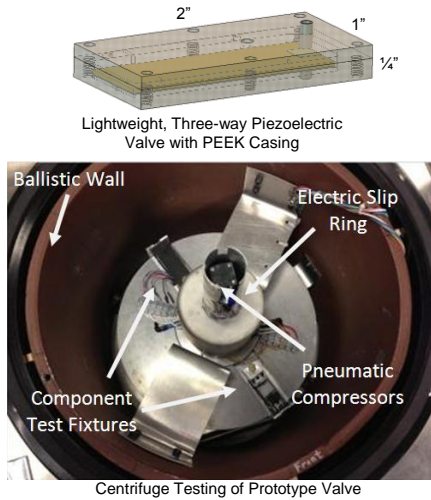


Figure 5. Piezoelectric valve design and centrifuge testing of valve under 500 g’s of CF loading.

Pneumatic Actuator Design

Based on the blade modification specifications provided to Invercon by Kaman, Invercon then designed a pneumatic actuator housing that would fit within the modified Control Box volume. A schematic of the resulting housing and actuator design, which underwent an internal design safety review by Kaman, is pictured in Figure 6. The actuator’s primary components are a pneumatic high pressure input line, a low pressure output line, three-way piezoelectric valves, two opposing actuating diaphragms, and a diaphragm dividing element that ultimately outputs rotational displacement and torque. The amount of resistive torque applied to the actuator output can be adjusted by changing the clamped length of the steel torque rod, thus readily providing a means to record multiple actuator performance points. The two sets of proportional valves control air flow into and out of the two opposing diaphragms, thus controlling the diaphragm pressures and the resultant actuator displacement and torque output. An angular sensor is used to measure actuator displacement, and two pressure sensors are used to monitor pressure levels in the high and low pressure lines, respectively. The total weight of the actuator parts is 1.3 lbs. Because this is an actuator feasibility test and because the scaled actuator must fit within a 12” blade span on a retrofitted blade, the resulting actuator torque output is also scaled down. Actuator torque, however, increases linearly with actuator length without sacrificing response time.

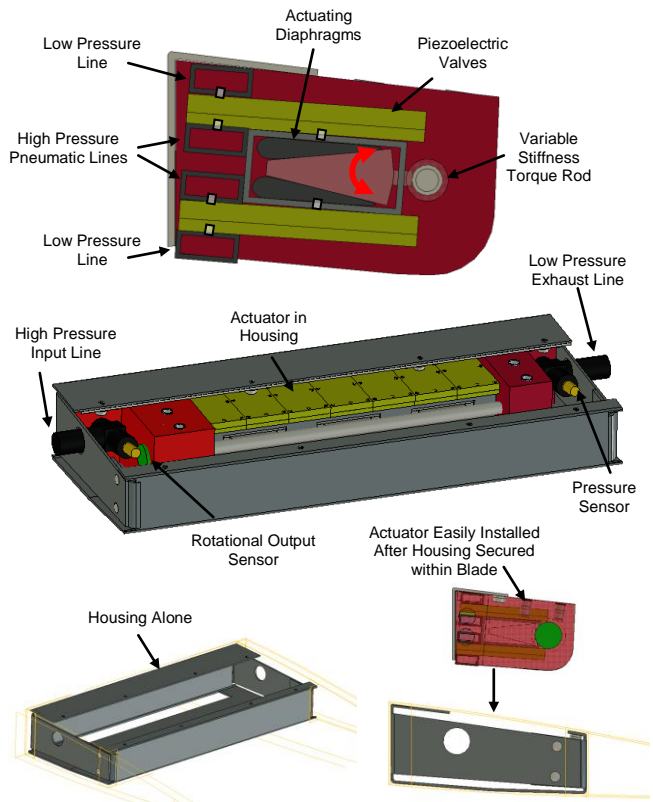


Figure 6. Pneumatic actuator and housing designed to fit within K911009 control box area

Spin Testing Setup at Kaman

The K-MAX blade modifications were conducted in Kaman’s blade shop, and the actuator design and actuator installation are pictured in Figure 7. In the figure, the installed high and low pressure lines can be observed. In Figure 8, the blade is installed on the whirl rig and the hardwired actuator is pictured along with the electronic control box placed at the hub center. The control box contains miniature electrical amplifiers that are powered with a +12 V signal and controlled with a low power 0-10V signal from the data acquisition system in the fixed frame. The amplifiers output the appropriate high voltage signals from 0 to +250 V to control valve flow to ultimately control the actuator output. A small pneumatic generator can also be observed in the box, and this device was used in the second phase of testing to determine the power harvesting potential of the pressure differential.

The actuator spin tests were a success, and the ability of the actuator to follow several complex command waveforms was demonstrated. In addition, the existence of a centrifugally generated pressure differential was again verified and measured. All spin tests were conducted at a blade rated 270 RPM. In Figure 9, representative data collection is plotted where the actuator rotational sensor output is plotted along with the actuator command signal vs. time. In the lower plot, the measured absolute pressure levels in the high and low pressure lines are plotted vs. time as the actuator is commanded. The maximum pressure

differential was recorded when both sets of valves were closed resulting in zero flow, and it was shown that the experimental pressure measurements were nearly perfectly predicted with the analytical model. The predicted and measured absolute pressures in the supply lines along with the pressure differential are plotted in Figure 10.

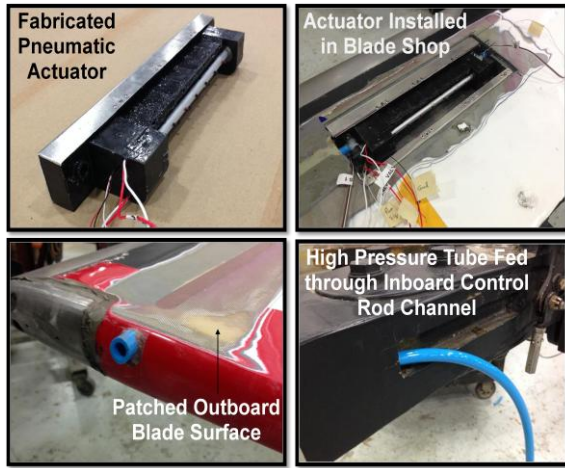


Figure 7. Actuator Installation in K-MAX Blade

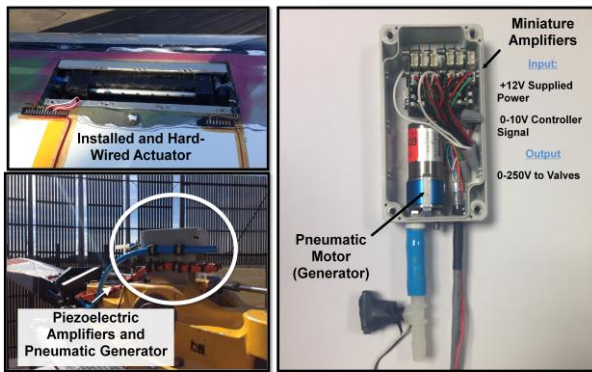


Figure 8. Valve power electronics and pneumatic generator located at hub center

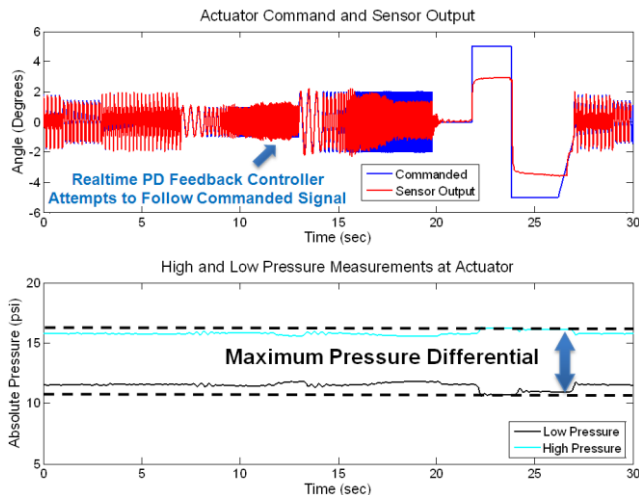


Figure 9. Representative spin testing results at 270 RPM, a) actuator rotation, b) pressure measurements

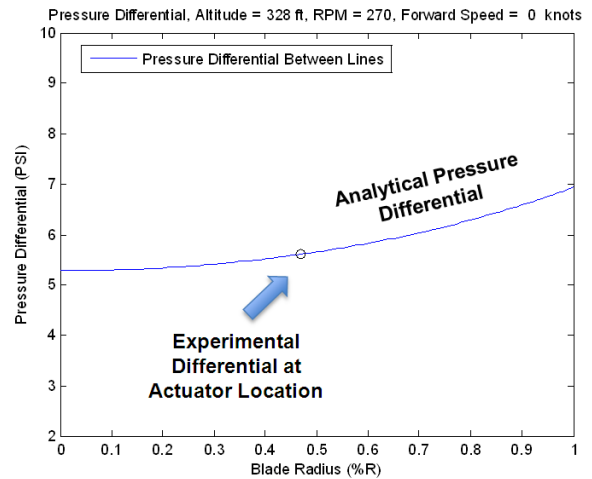
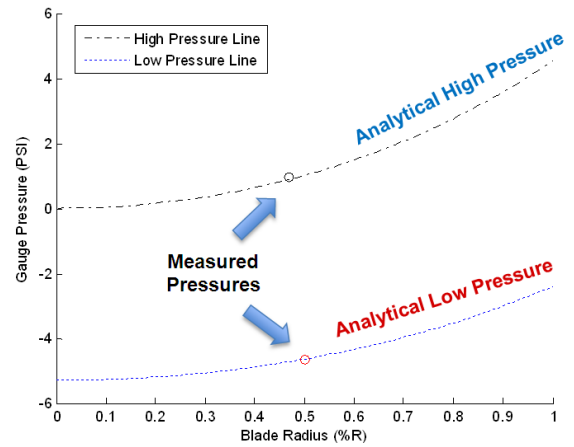


Figure 10. Experimental and analytical pressure differentials at actuator location at 270 RPM.

During spin testing data acquisition, the whirl rig slip ring introduced high frequency noise in the sensor data. Consequently during post processing, a low pass filter was used to eliminate frequency components above 60 Hz in the data. The time phase lag introduced by the filter was then subtracted to retain the original response time behavior of the actuator. This process is graphically demonstrated in Figure 11. It should be noted that the pressure signals were relatively noise free, and were thus not post processed.

For effective higher harmonic vibration control of rotorcraft, the highest actuation frequencies would need to be about 30 Hz. In Figure 11, a command case of $\pm 1^\circ$ at 30 Hz is plotted, and it is observed that the actuator can achieve $\pm 1^\circ$ of amplitude with only a 9 ms time lag. Because this time delay is constant and relatively small, it would likely be tolerable when considering feedback control algorithms, although this lag time can be reduced by using higher flow valves in the future. In Figure 13-Figure 15, example multi-frequency command cases are plotted along with their associated measured pressure differentials. All data was collected at 270 RPM, and it should be noted that the actuator had a physical stroke limitation of $\pm 4^\circ$. In the figures, multi-frequency cases are plotted along with the associated commands consisting of varying amplitude components at 5, 10, 15, and 20 Hz. In general, the results

display that the actuator is very responsive and can follow the multi-frequency commands. In addition, the pressure differential between the two lines is maintained at about 4.5 psi during high frequency actuation, indicating that the air flow through the actuator does not deleteriously affect source pressure levels. As will be demonstrated in the subsequent discussion, however, the maximum pressure differential can be maintained with a sufficiently large supply line diameter. The results suggest that actuator performance could be improved at higher frequencies by increasing air flow rates into and out of the actuating diaphragms, which further suggests that improved valve technology is required.

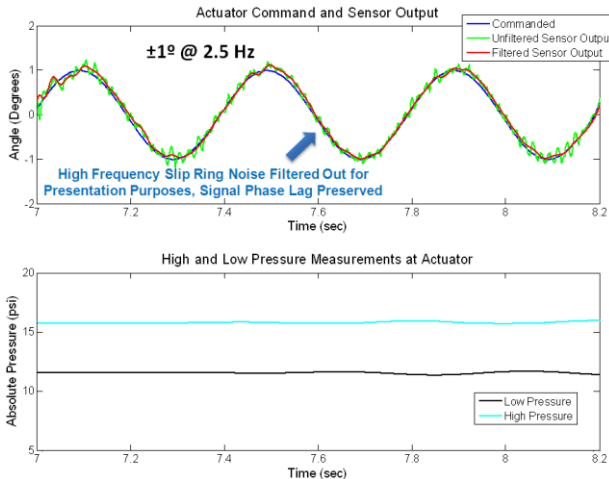


Figure 11. Demonstration of high frequency noise filtering of sensor output for plotting purposes

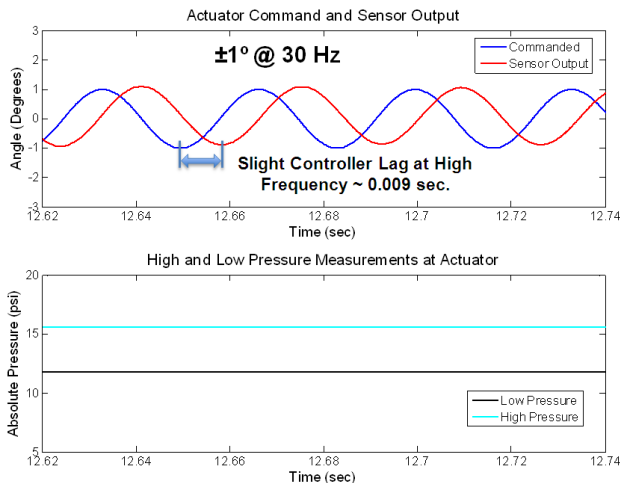


Figure 12. Command and measured output at $\pm 1^\circ @ 30 \text{ Hz}$ and accompanying pressure differentials at 270 RPM.

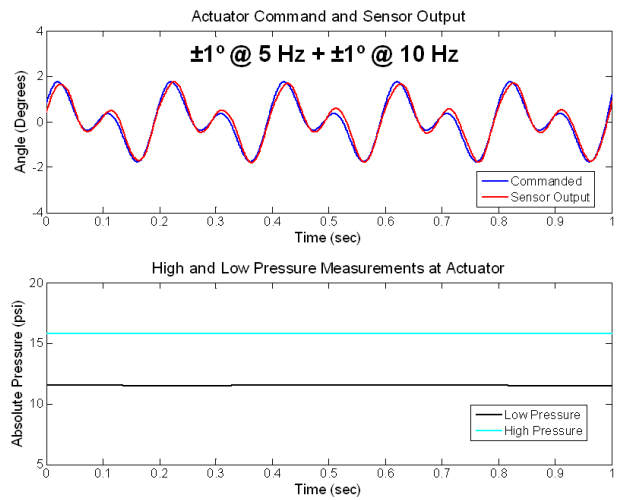


Figure 13. Multi-frequency commands and measured output and accompanying pressure differentials at 270 RPM.

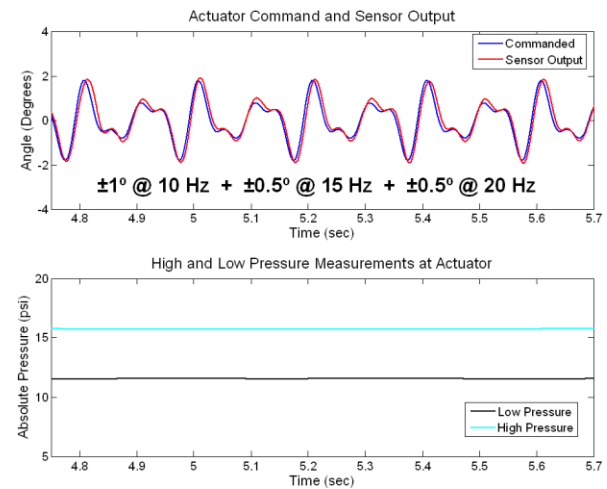


Figure 14. Multi-frequency commands and measured output and accompanying pressure differentials at 270 RPM.

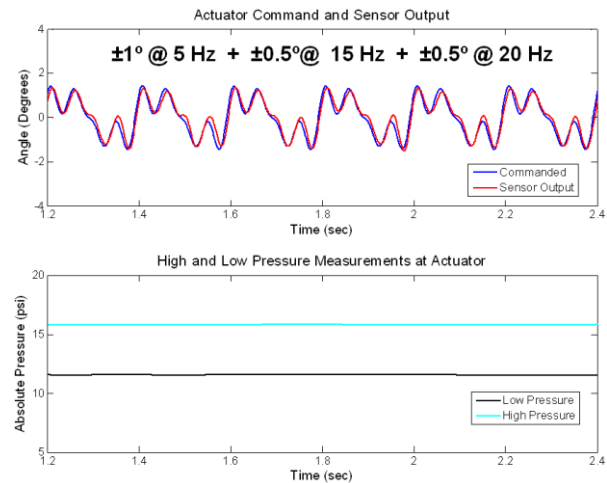


Figure 15. Multi-frequency commands and measured output and accompanying pressure differentials at 270 RPM.

Quasistatic and Dynamic Performance Testing

Comprehensive quasi-static and dynamic actuator performance tests were conducted where the pressure differential measured during spin testing was recreated in the laboratory to obtain detailed actuator performance metrics. For example, Figure 16 shows the results of quasistatic performance testing for increasing applied torque to the actuator output. It can be observed in the lower plot that target pressures were precisely recreated in each case. In Figure 17, a summary of both the quasistatic and dynamic cases is plotted, where the maximum achievable angular output is plotted against maximum applied torque. As expected, actuator torque and displacement output is increasingly diminished with frequency, with a roughly 25% decrease at 10 Hz, and a 75% decrease at 30 Hz. Although this particular pneumatic actuator is not necessarily optimized for flap actuation, a comparison can be made between this actuator’s performance and that of a piezoelectric-based actuator reported in the literature, Boeing’s double X-frame actuator. If the current 6” span actuator segment was increased to 30” (e.g., located behind a 45” flap), then the quasistatic performance would exceed that of the double X-frame. In Phase II, Invercon’s goal will be to improve the pneumatic actuator design to greatly exceed the current performance and significantly outperform all other flap actuation methods that exist today. This goal will be achieved by improving valve technology and ensuring that adequate flow is supplied to the next generation actuator.

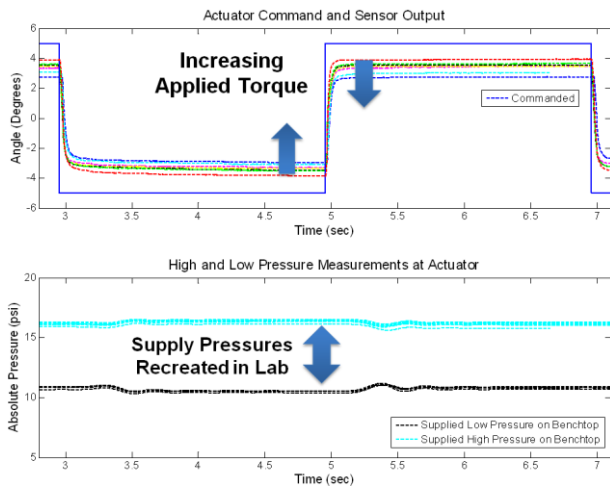


Figure 16. Actuator quasistatic performance testing data for increasing applied torque cases

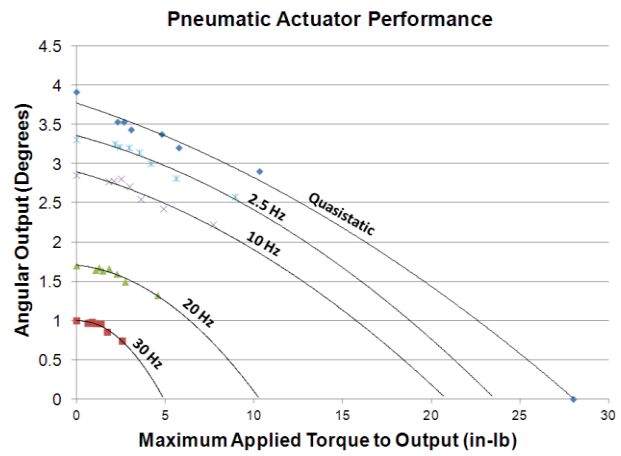


Figure 17. Summary of quasistatic and dynamic actuator performance

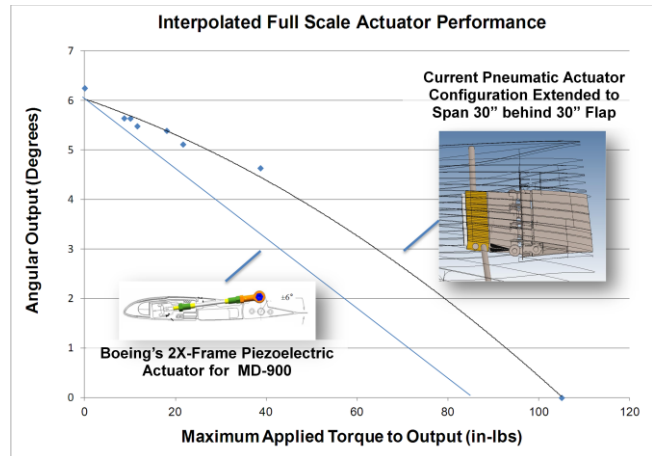


Figure 18. Interpolated performance of full-scale pneumatic actuator performance compared to piezoelectric actuator, 2X-frame.

Pneumatic Power Harvesting Results

Another innovation tested during the Phase I spin test was the potential to harvest electrical power using the CF generated pressure differential. In Figure 19, the power harvesting test configuration is pictured. The inboard, high pressure tubing inlet was first connected to the output of the pneumatic generator at the hub center. Then within the actuator housing, the tubing was re-routed so that it bypassed the actuator and spanned out to the blade tip. The effective result was a sealed volume spanning from the generator output to the blade tip. Upon spinning the rotor, a negative pressure is created which then turns the generator, thus generating electrical power. In the fixed frame, the generator voltage output was placed in parallel with a variable resistor. By measuring the voltage drop across the varying resistance, a power curve could be created (Figure 20) which would then indicate the maximum power that can be harvested from the system (using this particular generator). As shown in the figure, a maximum of 750 mW

can be continually harvested from the pneumatic line. This amount of power would be ample to run a wireless data transmitter and also power the piezoelectric valves proposed in Phase II.

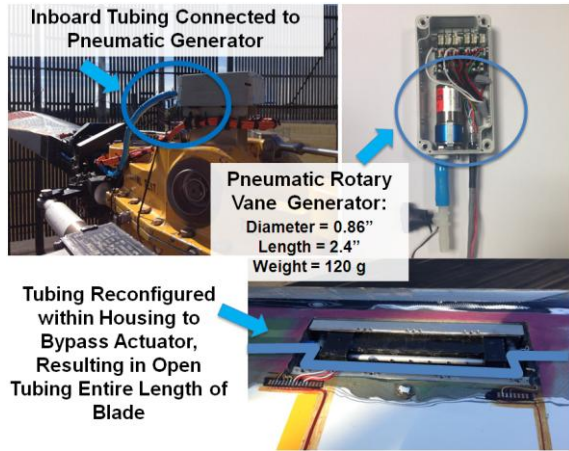


Figure 19. Pneumatic power harvesting spin testing configuration.

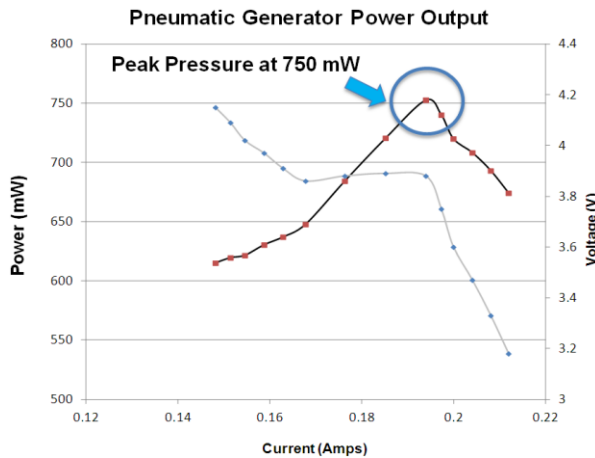


Figure 20. Pneumatic power harvesting results

Pressure and Flow Analysis

Supply Line Air Flow Analysis

When developing an actuator that relies on air flow resulting from a centrifugally developed pressure differential, it is instructive to examine the available flow through a pipe of a certain diameter given known pressure boundary conditions at the blade root and tip. It is assumed that the blade root air inlet has a constant pressure source equal to atmospheric pressure, p_{atm} . It is also assumed that the blade tip pressure, p_{tip} , is equal to atmospheric pressure plus the dynamic pressure due to the rotor tip speed:

$$p_{tip} = p_{atm} + C_p \left(\frac{1}{2} \rho V_{tip}^2 \right) \quad 1$$

where C_p is the pressure coefficient, ρ is the atmospheric air density, and V_{tip} is the blade tip speed. Based on previous spin tests to measure the pressure differential, a C_p value of

-1 is realistic, resulting in a negative tip gauge pressure. The Darcy-Weisbach equation can then be used to develop an expression to approximate the volumetric flow rate through the pipe, q , in terms of the pressure differential, Δp , pipe diameter, d , pipe length, L , and the pipe's Darcy friction factor, f_D .

$$q = \sqrt{\frac{2(\Delta p)d}{f_D L}} (A_{cross})$$

$$q = \sqrt{\frac{2(\Delta p)d}{f_D L}} \left(\frac{\pi d^2}{4} \right)$$

$$q = \sqrt{\frac{\pi^2 (\Delta p) d^5}{8 f_D L}} \quad 2$$

It is important to notice that the available flow to the actuator is directly proportional to $d^{5/2}$, implying that small increases to the diameter of the supply lines will result in sizeable increases in available air flow. Therefore, when designing such a pneumatic actuation system, it is important to maximize the cross-sectional pipe area to ensure sufficient air flow to the diaphragms.

Another important aspect of actuator design is to consider the air consumption requirements of the actuator and how that may impact the available pressure differential at the actuator location within the blade. To illustrate this point, consider a pneumatic actuator that employs an internal valve system that does not restrict air flow, or where the valve orifice's are sufficiently large so that there is no pressure drop across the valve. The two limiting operation conditions for the actuator will be when the supply flow is completely blocked, and when the actuator is operating at maximum frequency and maximum stroke, thus consuming the maximum amount of air flow. As an example, consider the K-MAX whirl test results previously presented. When flow is blocked through the actuator, or the valves are closed, then maximum pressure differential is achieved between the high and low lines, or about 6 psi. When there is unrestricted flow through the actuator, or essentially an open pipe from root to tip, then there will be a steady drop in pressure from the root to tip, resulting in a near zero pressure differential between the high and low pressure lines at the actuator location and maximum flow through the system. This example is presented graphically in Figure 21. Realistically, the actuator valve system will have some minimum pressure drop across it, but the assumption of unrestricted flow through the system provides a meaningful benchmark to guide supply line sizing. In general, it is a reasonable design guideline to size the supply lines so that when the actuator is operating at maximum frequency and stroke, the volumetric air consumption is no more than 10% of the maximum flow in the unrestricted case. Thus, when the actuator consumes the maximum amount of air, there will only be roughly a 10% drop in the available pressure differential between the high and low pressure lines.

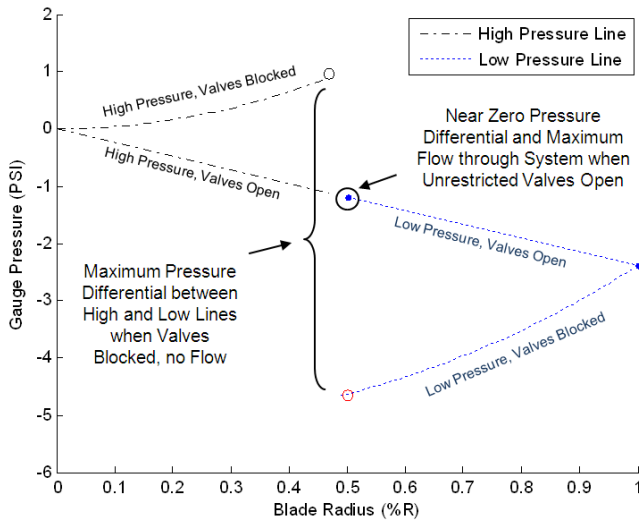


Figure 21. Illustration of how unrestricted flow through actuator results in zero pressure differential at actuator location.

As an example of the maximum pipe diameter that is required for a full-scale actuator, consider if the Phase I actuator were lengthened to 30” and actuated a 45” flap. In Figure 22, a side view of the Phase I diaphragms is shown with the actuator displaced both +5° and -5°. With one actuator stroke defined as one inflation and deflation cycle of both diaphragms corresponding to ±5°, then the total volume of air consumed in one stroke is calculated to be 6.33 in³. If the actuator needs to displace this much air thirty times a second, then the total air consumed by the actuator at 30 Hz would be 190 in³/s. In this case, the unrestricted air flow case would need to have a flow rate of at least 1,900 in³/s to satisfy the condition that the actuator consumes at most 10% of the maximum unrestricted flow rate in the supply lines. If Eq. 2 is solved for diameter:

$$d = \sqrt[5]{\frac{8q^2 f_D L}{\pi^2 (\Delta p)}} \quad 3$$

then the minimum diameter that would supply 1,900 in³/s would be 0.81 in., given the following parameters:

- q = 1900 in³/s
- f_D = 0.0189
- L = 24.11 ft.
- Δp = 5.53 psi

Therefore, the minimum diameter to provide sufficient flow to a pneumatic flap actuator operating at 30 Hz and ±5° is 0.81 inches, which is very feasible from a practical design standpoint.

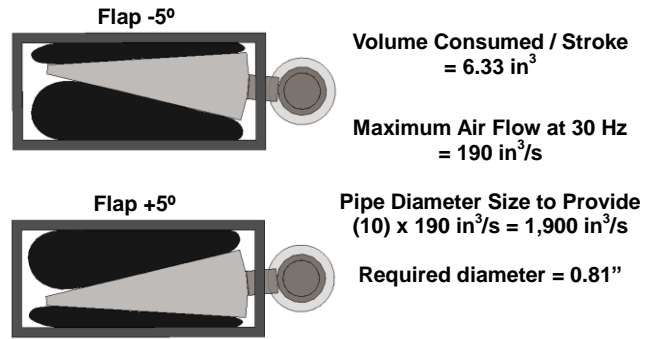


Figure 22. Maximum air consumption of full scale Phase I actuator at ±5° @ 30 Hz.

Pneumatic Diaphragm Actuator Modeling

Sufficient air flow is a critical design aspect to ensure that the actuator can operate successfully over all frequencies and amplitudes. Another crucial aspect to the design, however, is ensuring that the actuator valve system can deliver the necessary flow rates. Because it is a dynamic system with several variables to consider, it is necessary to develop a dynamic model of the actuator system ultimately to determine the minimum valve flow rates that are required to fully pressurize and depressurize the diaphragms at maximum frequency and amplitude.

Invercon has developed a preliminary pneumatic diaphragm actuator model in Simulink to accurately simulate the actuator dynamics. Figure 23 displays the actuator/flap model parameters, which include the flap angular displacement θ , aerodynamic stiffness k_{aero} , instantaneous pressures in the opposing diaphragms P_1 and P_2 , low and high pressure sources P_{low} and P_{high} , the instantaneous diaphragm volumes V_1 and V_2 , diaphragm lever arm r , resultant diaphragm forces F_1 and F_2 , flap moment of inertia I , and valve flow resistance, denoted as L_{ohms} , which is a useful valve parameter developed by valve manufacturer, The Lee Company, to characterize a valve’s flow resistance.

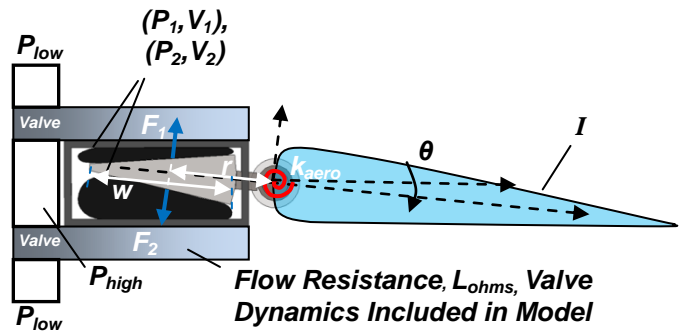


Figure 23. Schematic of pneumatic diaphragm actuator model parameters. Valve dynamics also modeled.

The equation of motion for the flap can be expressed as:

$$I\ddot{\theta} + c_{aero}\dot{\theta} + k_{aero}\theta = F_1r - F_2r \quad 4$$

where c_{aero} is effective aerodynamic damping, and F can be calculated using the expression:

$$F = PA_{eff} \quad 5$$

where A_{eff} is the effective area over which the pressure acts. The instantaneous volume of the diaphragms can be approximated with:

$$\begin{aligned} V_1 &= V_o + rw\theta \\ V_2 &= V_o - rw\theta \end{aligned} \quad 6$$

Where V_o is the volume in the diaphragms at $\theta = 0$. The change in volumes with respect to time is simply:

$$\begin{aligned} \dot{V}_1 &= rw\dot{\theta} \\ \dot{V}_2 &= -rw\dot{\theta} \end{aligned} \quad 7$$

The ideal gas law can be used to approximate the relationship between changes in pressure, volume, and temperature in both diaphragms:

$$PV = \frac{m}{M} RT \quad 8$$

where m is the mass of air in the diaphragm, M is the molar density of air (28.97 g/mol), R is the gas constant ($R = 8.314 \text{ m}^3\text{Pa/K/mol}$), and T is the temperature, which is assumed to stay constant at 70° for the purposes of this simulation.

The rate of change of the pressures in each diaphragm can be approximated by taking the time derivative of the relationship in Eq. 8.

$$\begin{aligned} \dot{P}V + P\dot{V} &= \frac{\dot{m}}{M} RT \\ \dot{P} &= \frac{\frac{\dot{m}}{M} RT - P\dot{V}}{V} \end{aligned} \quad 9$$

Finally, the mass flow rate is governed by the flow resistance of the valves and the existing pressure differential, either between P_1 and the low or high pressure, or between P_2 and the low or high pressure. The following expression has been developed by The Lee Company to calculate a valve's resistance to fluid flow, explicitly:

$$L_{ohms} = \frac{2K\sqrt{\Delta PP_{downstream}}}{\dot{m}/\rho} \quad 10$$

where K is a constant that varies with the type of gas. The mass flow rate into or out of the diaphragms can easily be

determined from this relationship, depending on the existing pressure differential direction:

$$\dot{m} = \frac{2\rho K\sqrt{\Delta PP_{downstream}}}{L_{ohms}} \quad 11$$

Based on these relationships, a state model was constructed and modeled using SIMULINK. It should be noted that valve dynamics were also included in the model, where the valve response time was limited to 5 ms, corresponding to response times of piezoelectric benders.

Actuator/Flap Model Validation

The actuator/flap model was validated using the experimental Phase I results from the spin test. In Figure 24 - Figure 28, the model analytical performance is overlaid on the experimental results for the various spin test command cases. It can be observed that for all cases, the model captures the Phase I system dynamics very accurately. Given the flow restrictions of the valves used in the Phase I tests, the high frequency lag time between the actuator output and command signal is captured very well, as shown in Figure 24 and Figure 25. Moreover, the multi-frequency command cases are also modeled accurately as observed in Figure 26 - Figure 28. Now that a validated model was completed, it was now possible to vary the model parameters to investigate the feasibility of powering full-scale flaps with the centrifugally powered pneumatic concept. As a result, both the ability to power flap for higher frequency vibration control and primary rotor control could now be investigated.

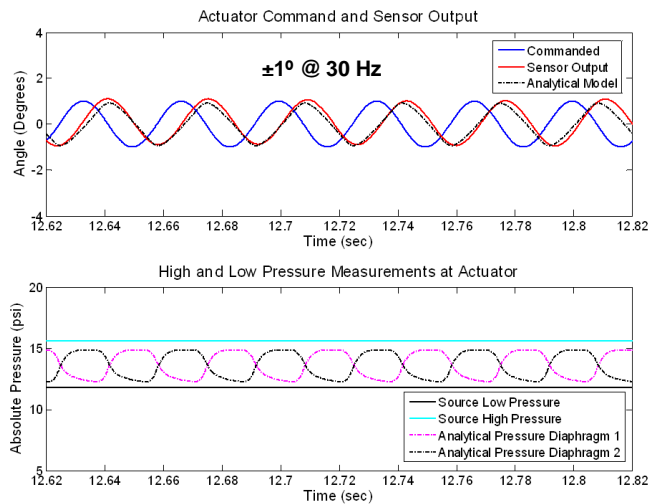


Figure 24. Spin test results at 270 RPM, a) Experimental and analytical actuator output for $\pm 1^\circ @ 30 \text{ Hz}$ b) Associated analytical pressures in diaphragms

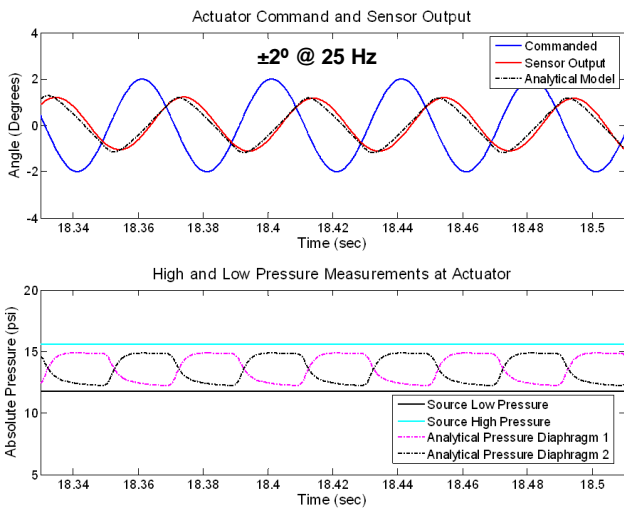


Figure 25. Spin test results at 270 RPM, a) Experimental and analytical actuator output for $\pm 2^\circ @ 25 \text{ Hz}$ b) Associated analytical pressures in diaphragms

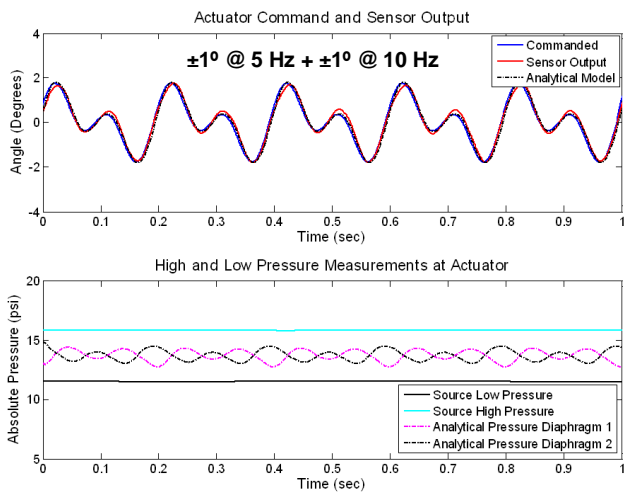


Figure 26. Spin test results at 270 RPM, a) Experimental and analytical actuator output for $\pm 1^\circ @ 5 \text{ Hz} + \pm 1^\circ @ 10 \text{ Hz}$ b) Associated analytical pressures in diaphragms

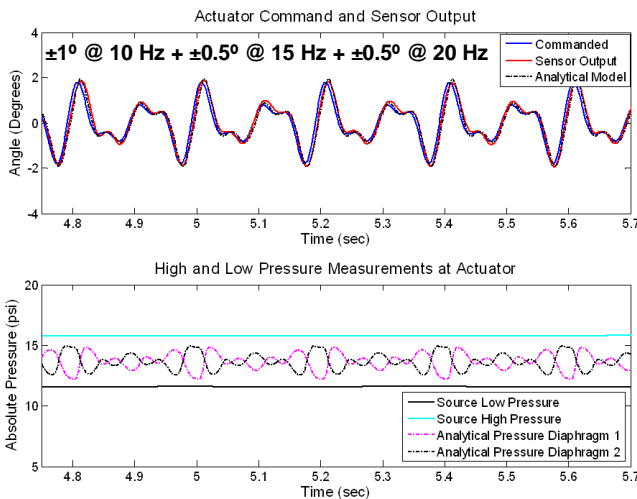


Figure 27. Spin test results at 270 RPM, a) Experimental and analytical actuator output for $\pm 1^\circ @ 10 \text{ Hz} + \pm 0.5^\circ @ 15 \text{ Hz} + \pm 0.5^\circ @ 20 \text{ Hz}$ b) Associated analytical pressures in diaphragms

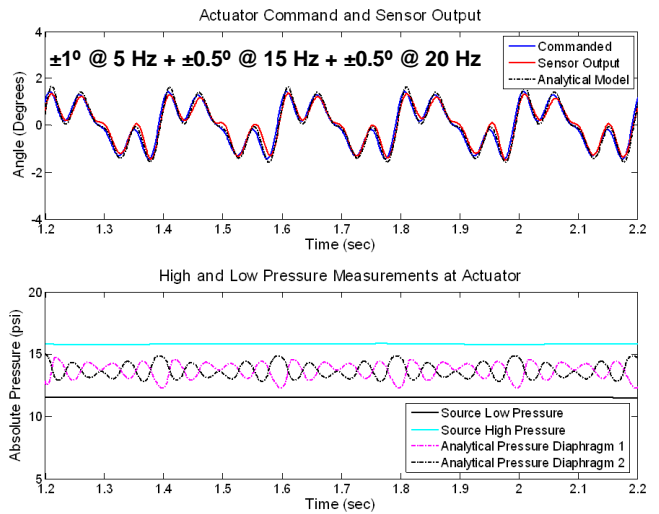


Figure 28. Spin test results at 270 RPM, a) Experimental and analytical actuator output for $\pm 1^\circ @ 5 \text{ Hz} + \pm 0.5^\circ @ 15 \text{ Hz} + \pm 0.5^\circ @ 20 \text{ Hz}$ b) Associated analytical pressures in diaphragms

Feasibility Study of Power Trailing Edge Flaps using Validated Actuator/Flap Model

With the validation of the actuator/flap dynamic model, it is now possible to predict the performance of realistic pneumatic actuator systems for powering trailing edge flaps for both vibration control and primary rotor control. In all of the subsequent example cases, it is assumed that the modeled pneumatic actuator systems are powering a trailing edge flap sized for a Bell Model 430 helicopter, as outlined in Ref. 7. In Ref. 7, the flap parameters are given as the following:

- Flap Length = 45"
- Flap Inertia = 5.8 lb-in²
- Flap Aerodynamic Stiffness = 18 in-lb/deg
- Frequency Range = 5.8 Hz to 29 Hz

These flap parameters were incorporated into the model, and the actuator parameters were then adjusted within realistic limits to demonstrate the performance limits of pneumatic flap actuation. In all of the subsequent cases, the maximum pressure differential was assumed to be that as measured in the Phase I spin tests, or a differential of 5.53 psi, which is a conservative assumption for the Model 430 rotor.

In Figure 29, the analytical performance results for a 30" actuator powering the Model 430 flap are plotted. The command signal is $\pm 5^\circ @ 30 \text{ Hz}$. The results assume that the actuator valves have about 25% the flow resistance as those used in the Phase I test, which is a feasible design assumption. The chordwise geometry of the actuator is assumed to be the same as the Phase I actuator. As observed in the figure, the actuator is capable of oscillating the flap $\pm 5^\circ$ at 30 Hz, which would be adequate for higher harmonic vibration control. For this particular case, the model predicts that the actuator consumes an average

volumetric flow rate of $190 \text{ in}^3/\text{s}$. Using our design requirement developed above that the flow of the unrestricted flow case be 10X the flow consumed by the actuator, then the unrestricted flow rate would need to be $1,900 \text{ in}^3/\text{s}$. Using Eq. 3, the pipe diameter to ensure this flow rate would be $0.81''$, which is entirely feasibly for this size rotor blade. A similar case is shown in Figure 30, where all model conditions are the same except the command signal is now multi-frequency, $\pm 1^\circ @ 10 \text{ Hz} + \pm 2^\circ @ 20 \text{ Hz} + \pm 3^\circ @ 30 \text{ Hz}$. This case demonstrates that the actuator would be capable of following more realistic multi-frequency commands. For this case, the actuator consumes slightly more volume with an average rate of $200 \text{ in}^3/\text{s}$, which corresponds to a required pipe diameter of $0.82''$.

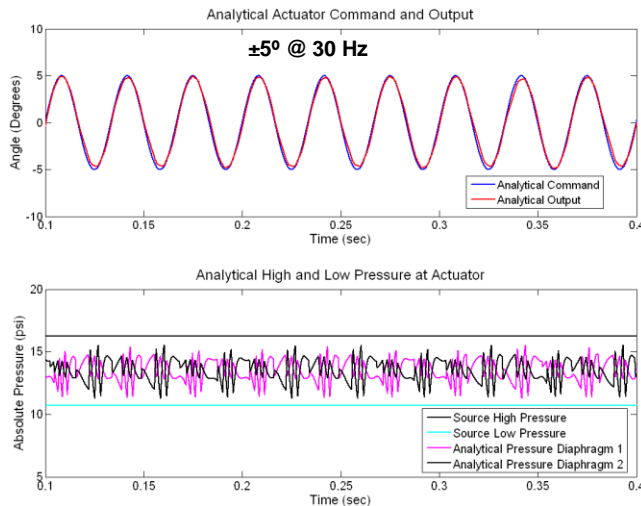


Figure 29. Analytical performance results for a 30” pneumatic actuator powering Model 430 flap at $\pm 5^\circ @ 30 \text{ Hz}$, same chordwise geometry as Phase I actuator, valves have 25% flow resistance as Phase I valves

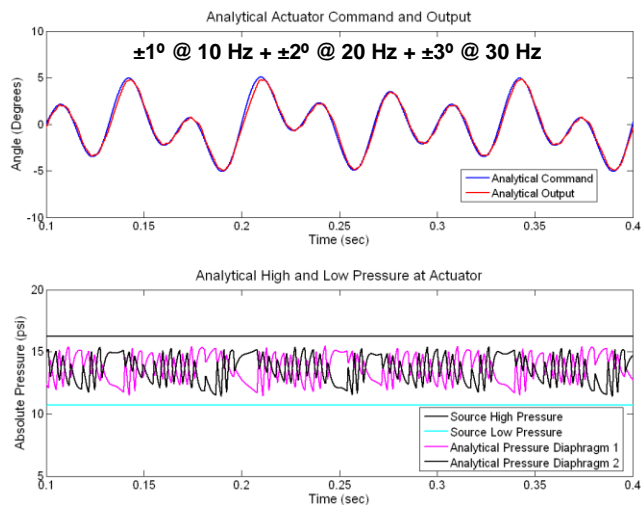


Figure 30. Analytical performance results for a 30” pneumatic actuator powering Model 430 flap at $\pm 1^\circ @ 10 \text{ Hz} + \pm 2^\circ @ 20 \text{ Hz} + \pm 3^\circ @ 30 \text{ Hz}$, same chordwise geometry as Phase I actuator, valves have 25% flow resistance as Phase I valves

Another interesting case to investigate is the possibility of providing very high flap displacements to enable primary rotor control. In the following cases, the actuator length is again $30''$. The actuator chordwise geometry was slightly adjusted so that the $r = 1.5''$ and $w = 1.1''$ corresponding to the parameters shown in Figure 23. In addition, the value of V_0 was increased to correspond to diaphragm volumes that can accommodate large displacements of $\pm 20^\circ$. In Figure 31, the command case of $\pm 20^\circ @ 6 \text{ Hz}$ is shown, which is the actuating condition that would be required for swashplateless control. For this case, the valve resistance would need to be reduced to 10% that of the Phase I actuator. The actuator would consume an average volumetric flow rate of $290 \text{ in}^3/\text{s}$, which is understandably higher than the previous cases. The required pipe diameter would then need to be increased to $0.91''$, which would still remain a realistic design value. In Figure 32, the results of a similar case are shown where the command signal is now $\pm 6^\circ @ 30 \text{ Hz} + \pm 14^\circ @ 6 \text{ Hz}$, which would correlate to swashplateless rotor control with additional higher harmonic vibration control. In order for the actuator to sufficiently follow the command signal, the valves would need to have a flow resistance that is 6% of those used in the Phase I actuator. Such valving requirements are planned to be developed in Phase II. As shown in the figure, such an actuator would be capable of providing significant flap motion and would consume $422 \text{ in}^3/\text{s}$, which corresponds to a pipe diameter of $1.09''$, which again is a realistic design value for this size rotor blade.

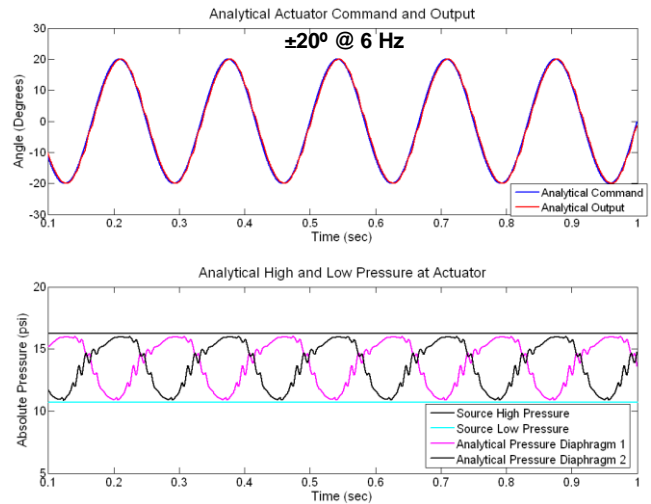


Figure 31. Analytical performance results for a 30” pneumatic actuator powering Model 430 flap at $\pm 20^\circ @ 6 \text{ Hz}$, actuator chordwise geometry slightly adjusted within feasible limits, valves have 10% flow resistance as Phase I valves

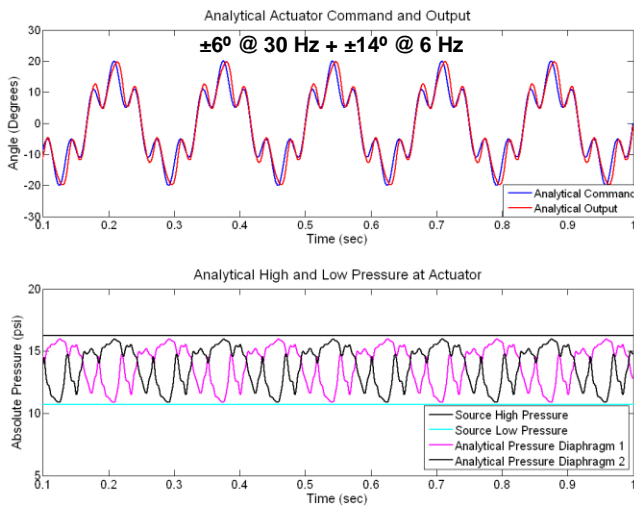


Figure 32. Analytical performance results for a 30” pneumatic actuator powering Model 430 flap at ±6° @ 30 Hz + ±14° @ 6 Hz, actuator chordwise geometry slightly adjusted within feasible limits, valves have 6% flow resistance as Phase I valves

Pneumatic Actuator Stiffness Analysis

In order to maintain flap displacements as prescribed by a control algorithm, it is critical that the actuation system be as stiff as possible to withstand any unsteady aerodynamic forcing and to resist deflection under particularly high aerodynamic loading. The pneumatic actuator stiffness can be calculated by considering the pressurized diaphragms as air springs. The following equation is a common expression to calculate the stiffness of an air spring:

$$k_{airspring} = \frac{[nA_{eff}^2 (p^{gauge} + p^{atm})]}{V} \quad 12$$

In this equation, n is the gas constant (1.4 for air), A_{eff} is the effective diaphragm area over which a force acts, p^{gauge} is the gauge pressure, p^{atm} is the atmospheric pressure, and V is the diaphragm volume. In the case of the pneumatic flap actuator, a nominal flap stiffness can be calculated when the flap has zero deflection. For the pneumatic diaphragm pictured in Figure 33, the parameters would have the following values:

$$V = 3^\circ (\pi/180^\circ) rwL$$

$$V = 3^\circ (\pi/180^\circ)(0.8'')(1'')(30'') = 1.26 \text{ in}^3$$

$$A_{eff} = (30) * (1) = 30 \text{ in}^2$$

$$p^{atm} = 14.69 \text{ psi}$$

$$p^{gauge} = 1.55 \text{ psi}$$

Therefore,

$$k_{eff} = [(1.4)30^2(16.24)]/1.26 = 16,240 \text{ lb/in} = 2,844,000 \text{ N/m}$$

From a rotational perspective, the diaphragm can be assumed to act with an effective 0.8” lever arm from the hinge location. Therefore, the rotational stiffness of the actuation system can be approximated by assuming small angular displacements:

$$k_\theta = 10,400 \text{ lb*in/rad} = 1,170 \text{ N*m/rad}$$

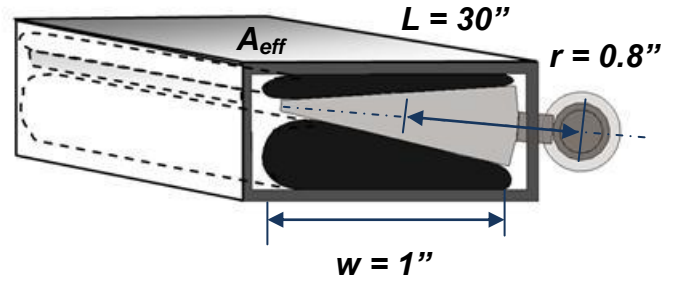


Figure 33. Calculation of pneumatic actuator stiffness for 30” pneumatic actuator in KMAX blade.

As a comparison of actuator stiffnesses, the rotational stiffness of the pneumatic actuator can be compared to that of Boeing’s piezoelectric 2X-frame flap actuator. The mechanical rotational stiffness of the 2X-frame can be estimated by examining schematics in Ref. 8, pictured in Figure 34. As observed in Figure 34, the linear output of the actuator is offset from the flap hinge using a lever arm of 0.75”. Assuming the authors were successful in designing a linear actuator with a target stiffness of ~1000 lb/in, then the rotational stiffness of the system can be estimated to be 375 lb*in/rad. **Therefore, the rotational stiffness of the proposed pneumatic actuation system would be on the order of 40 times that of the state-of-the-art piezoelectric 2X-frame actuation system in the zero angle position.**

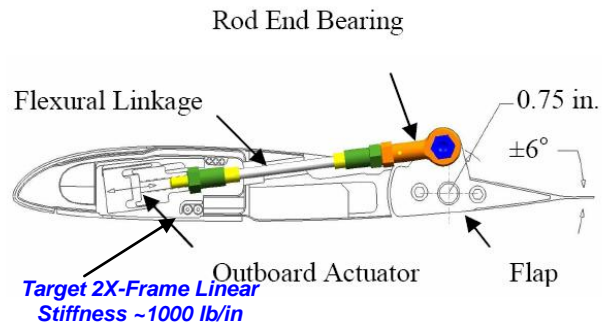


Figure 34. Boeing’s 2X-Frame geometry and stiffness⁹

Future Test Plans

In order to improve actuator performance at higher frequencies, it is evident that the valve technology must be improved to enable higher flow rates. One method to achieve higher flow through the valves is through the use of piloted valve technology. In Figure 35, a schematic of a

high flow, piloted piezoelectric valve is shown. Instead of the piezoelectric bender controlling flow into and out of the diaphragm, it instead controls flow into a small volume within the valve that causes a piston to move, which then in turn opens high flow orifices to either the high or low pressure sources.

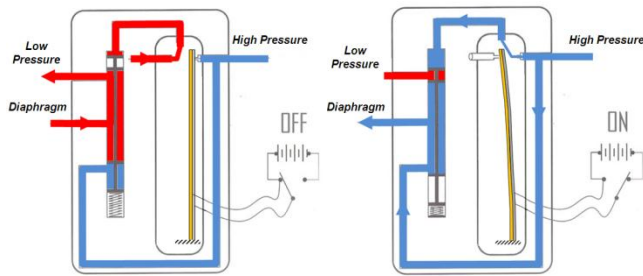


Figure 35. Basic example of piloted valve technology for flow amplification.

However, a piston-based, piloted valve like that shown in Figure 35 would typically not operate properly in the extremely high centripetal acceleration it would experience on a rotor blade. Therefore, a specialized piloted valve design would need to be developed that could deliver high flow to the pneumatic actuator diaphragms under extreme CF. In Figure 36, a schematic of a conceptual, next generation actuator system is shown which incorporates piloted valve technology. The purpose of this schematic is to demonstrate a feasible actuator system incorporating a piloted valve system and is not necessarily the type of design that would be pursued in Phase II. As shown in the figure, the actuator consists of four, inboard, pilot valves which would control air flow into and out of small, amplifier diaphragms. Depending on the given pressure levels in the opposing diaphragms, long channel orifices would be opened or closed to connect the main diaphragms to either the main low pressure line or the main high pressure line. Because relatively large orifices would be opened quickly, the main diaphragm pressures could be rapidly adjusted, which would eliminate the need for all of the air flow to pass through the piezoelectric valves alone. Conservatively, the valve orifice size could be increased by over a factor of 50 as compared to just using the piezoelectric valves, which would dramatically improve actuator higher frequency performance and enable the analytical cases presented above.

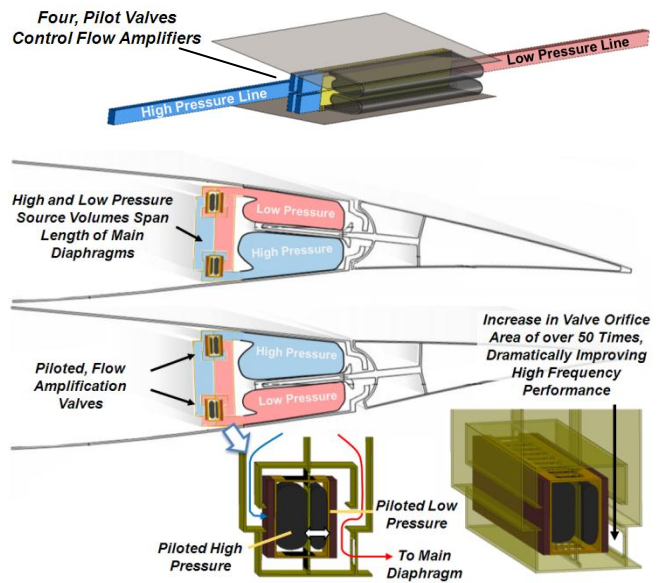


Figure 36. Conceptual schematic of next generation actuator incorporating high flow, piloted valve technology

As an example of the projected performance improvements that could be achievable with a pneumatic actuator, Figure 37 shows another actuator design embodiment which incorporates the piloted valve technology and also a bellows-type diaphragm design. This design assumes that a 30" actuator would be placed directly in front of the flap, with an effective 2" lever arm from the center of the diaphragms to the flap axis, and a 1" length over which the diaphragms act on the lever arm. This design assumes that the diaphragms will maintain full contact with the lever arm throughout the entire stroke. Because a bellows type diaphragm is utilized, the area over which the pressure acts remains constant over the actuator's entire stroke. If this is the case, then this implies that the torque output is not stroke limited, which is why the full output torque could be achieved even at very high displacements. If this design can be successfully implemented, it could potentially enable washplateless rotors where primary control is provided entirely by flaps because of the very high actuator displacements and torques.

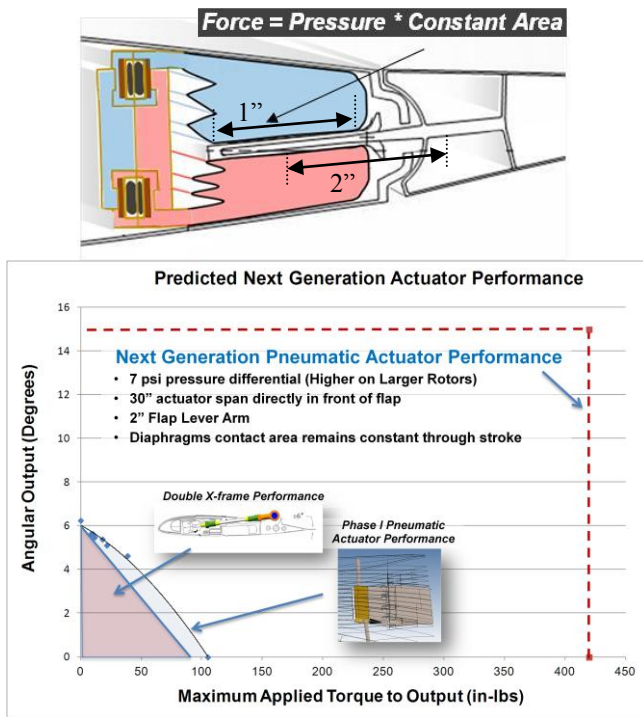


Figure 37. Comparison of predicted next generation actuator performance compared to Phase I actuator and 2X-frame actuator performance.

A graphical representation of the planned future spin testing is pictured in Figure 38. The blades originally modified in Phase I can be utilized to conserve project resources. The Phase I actuator will be replaced by a next generation actuator that incorporates piloted valve technology. All of the power required to operate actuator valves and sensors will be produced using a pneumatic energy harvester located at the hub. Additionally, a wireless transmitter that can transmit up to 500 samples per second will also be powered using harvested energy. The transmitter will be used in lieu of the mechanical slip ring to control the actuator from the fixed frame. The overall goal is to demonstrate the enabling technology for a self-powered, wirelessly controlled actuation system that could eventually be used to enable swashplateless rotors; a long held pursuit within the rotorcraft community.

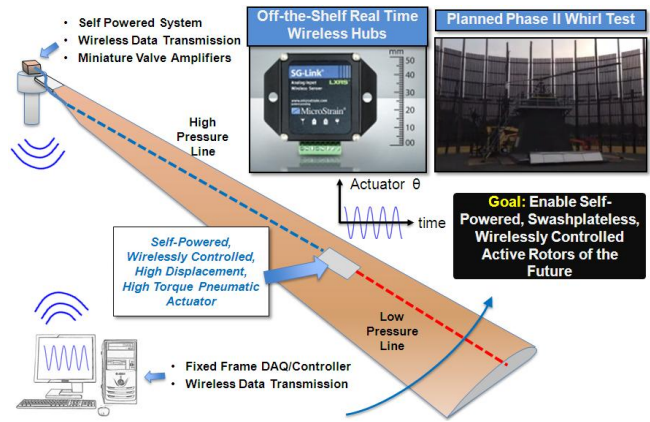


Figure 38. Planned future testing of wireless, self-powered, next generation actuation system

Current TRL: TRL 4

Applicable Programs/Projects

Subsequent to the current award, Invercon was chosen by Sikorsky Aircraft to support DARPA’s “High Speed Rotorcraft Test program” (Prime Contract FA8650-13-C-7304). Invercon has been subcontracted to fabricate, test and deliver full-scale pneumatic Miniature Trailing edge Effector (MiTE) cartridges, which will be powered using Invercon’s centrifugally powered pneumatic concept. The scaled, high speed rotor will ultimately be wind tunnel tested in the NASA Ames NFAC facility. The current NASA program will help validate the general actuation concept on a full-scale rotor prior to the scaled rotor, NFAC tests. In addition, Invercon is collaborating with Bell Helicopter to investigate the use pneumatic actuators to power trailing edge flaps.

Publications and Patent Applications

Paper accepted to the 2014 American Helicopter Society Conference in Montreal, Canada.

Patent:
 US Patent Title: “Pneumatic Actuator System for a Rotating Blade” Inventor: Dr. Joseph Szefi, Invercon, LLC
 Filing Date: February 3rd, 2011

References

- ¹ Yeo, H., and Chopra, I., “CFD-CSD Analysis of Active Control of Helicopter for Performance Improvement,” American Helicopter Society 65th Annual Forum Proceedings, Grapevine, TX, May 27-29, 2009.
- ² Shen, J., and Chopra, I., "Swashplateless Helicopter Rotor System with Trailing- Edge Flaps for Flight and Vibration Controls," Journal of Aircraft, Vol 43, No. 2, Apr-May 2006, pp. 346-352
- ³ Bluman, James, E., “Reducing Trailing Edge Flap Deflection Requirements in Primary Control through a Moveable Horizontal Tail,” Aerospace Engineering, PSU Master’s Thesis, 2008.
- ⁴ Chopra, I., Shen, J., “Actuation Requirements of Swashplateless Trailing-Edge Flap Helicopter Rotor in Maneuvering and Autorotation Flights” AHS 60th Annual Forum, Baltimore, Maryland, June 7-10, 2004
- ⁵ Duling, C. Gandhi, F., Straub, F., “On Power and Actuation Requirement in Swashplateless Primary Control using Trailing-Edge Flaps”, AHS 66th Annual Forum, Phoenix, Arizona, May 11-13, 2010.
- ⁶ Shen, J., Chopra, I., Johnson, W., “Performance of Swashplateless Ultralight Helicopter Rotor with Trailing-Edge Flaps for Primary Flight Control,” AHS Forum 59, Phoenix, AZ, 2003.
- ⁷ Shank, T.C., Szefi, J.T., Kothera, C.S., “ Comparative Bench Test Assessment of Medium Authority On-blade Actuation Technologies,” Presented at the American Helicopter Society 70th Annual Forum, Montreal, Canada, May 20-22, 2014.
- ⁸ Straub, F.K., Kennedy, D.K., “Design, Development, Fabrication and Testing of an Active Flap Rotor System,” Presented at the American Helicopter Society 61st Annual Forum, Grapevine, TX, June1-3, 2005.
- ⁹ Straub, F.K., Kennedy, D.K., “Design, Development, Fabrication and Testing of an Active Flap Rotor System,” Presented at the American Helicopter Society 61st Annual Forum, Grapevine, TX, June1-3, 2005.